A Transition State Analogue for the Oxidation of Binuclear Palladium(II) to Binuclear Palladium(III) Complexes

A Transition State Analog for the Oxidation of Binuclear Pd(II) to Binuclear Pd(III) Complexes

David C. Powers and Tobias Ritter*

Department of Chemistry and Chemical Biology, Harvard, University, 12 Oxford Street, Cambridge, MA, USA. Tel: 617 496 0750; Fax: 617 496 4591

ABSTRACT: Cooperative metal–metal (M–M) redox chemistry has the potential to lower activation barriers for redox transformations relevant to catalysis. Pd_2(III,III) complexes, generated by oxidation of Pd_2(II,II) complexes, have recently been implicated as intermediates in a variety of Pd-catalyzed C–H oxidation reactions. M–M redox synergy, mediated by Pd–Pd bond formation and cleavage, has been proposed to facilitate both oxidation and reductive elimination steps during various Pd-catalyzed directed C–H oxidation reactions. Herein, we report a transition state mimic for the oxidation of Pd_2(II,II) complexes which suggests that M–M redox synergy is involved in the oxidation of Pd_2(II,II) complexes to Pd_2(III,III) complexes.

Polynuclear transition metal assemblies are frequently encountered in the active sites of metalloenzymes that are responsible for redox catalysis in Nature.[1] For example, enzyme-bound binuclear Cu and Fe sites effect the partial oxidation of methane to methanol in methane monooxygenases.[1a,d,e] Information regarding substrate interactions with enzyme active sites can be derived from transition state analogs, which are structures in which a small molecule that is structurally similar to the endogenous enzyme substrate, but chemically inert toward the enzyme, is bound to the active site.[2] In comparison to biological redox chemistry, polynuclear transition metal catalysts are less frequently studied in synthetic catalysis systems. Recently, binuclear intermediates have been implicated in a variety of Pd-catalyzed C–H functionalization reactions (i.e. Fig. 1).[3] Bimetallic redox synergy, accomplished by Pd–Pd bond formation during oxidation of Pd_2(II,II) complexes to Pd_2(III,III) complexes, and Pd–Pd bond cleavage during subsequent product-forming C–X reductive elimination, has been proposed to facilitate redox transformations in some $Pd(OAc)_2$-catalyzed C–H oxidation reactions.[3g] Herein, we report a transition state analog for the oxidation of binuclear Pd(II) complexes to binuclear Pd(III) complexes, in which tetracyanoethylene, a potent electron acceptor, is bound to a dipalladium complex. This structure allows visualization of the interaction of binuclear Pd complexes with electron acceptors at an intermediate point on the Pd_2(II,II) to Pd_2(III,III) reaction coordinate and highlights nascent Pd–Pd bonding interactions during oxidation of binuclear Pd(II) complexes.

Binuclear Pd(III) intermediates have been proposed as intermediates in C–C,[3b] C–O,[3c] C–Cl,[3a,d] and C–CF_3 bond-forming reactions.[3h] Oxidation of Pd_2(II,II) complexes[5] can afford binuclear Pd(III) complexes with Pd–Pd bonds, formed by removal of two electrons from the Pd–Pd σ* orbital (Fig. 2).[3g,6] Measurements of reaction kinetics of $Pd(OAc)_2$-catalyzed C–H arylation[3b] and chlorination[3a,d] have suggested that oxidation during catalysis involves binuclear intermediates (Fig. 1). Reductive elimination from binuclear Pd(III) complexes results in reduction of Pd(III) to Pd(II) and accomplishes Pd–Pd bond cleavage. Investigation of the stoichiometric organometallic

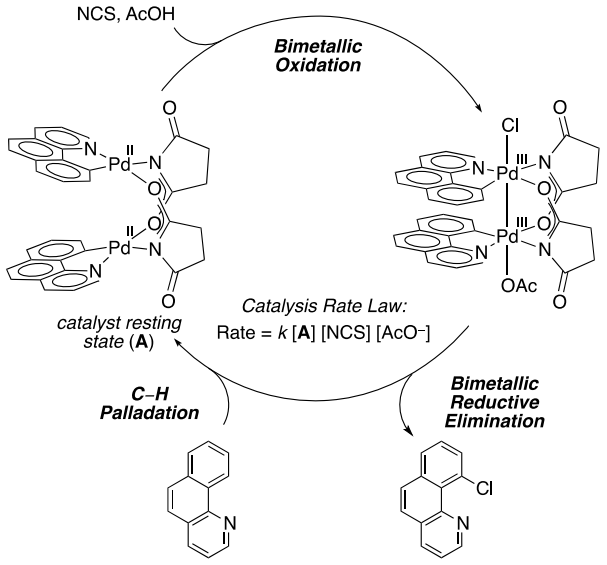

Figure 1. Catalysis cycle for $Pd(OAc)_2$-catalyzed chlorination of benzo[*h*]quinoline proceeds via oxidation of Pd_2(II,II) resting state **A** to a Pd_2(III,III) intermediate,[4] from which bimetallic C–Cl reductive elimination proceeds.

reactions of independently synthesized and isolated binuclear Pd(III) chlorides has shown that C–Cl reductive elimination proceeds without fragmentation of the binuclear core.[3a,e]

We have been interested in the hypothesis that M–M redox synergy can lower activation barriers to both oxidation of Pd_2(II,II) to Pd_2(III,III) and reductive elimination from Pd_2(III,III) complexes.[3g] As such, understanding the role of M–M bond formation and cleavage, and attendant perturbation of the Pd–Pd distance, during redox transformations relevant to catalysis is crucial. We have proposed that nascent Pd–Pd bonding interactions in the oxidation transition state can provide a lower-barrier process for metal-centered oxidation reactions than for monometallic oxidation:[3g] During monometallic oxidation, the oxidant X–Y bond is cleaved and new Pd–X and Pd–Y bonds are formed, while during a bimetallic oxidation, the same X–Y bond is cleaved and Pd–X and Pd–Y bonds are formed, but in addition, a Pd–Pd bond is formed

(Fig. 2).[6] In this Communication, we report a transition state analog for oxidation of Pd_2(II,II) complexes, which reveals Pd–Pd contraction upon coordination of an electron acceptor to the binuclear core of **1**, which is consistent with partial Pd–Pd bond formation during oxidation of Pd_2(II,II) complexes to Pd_2(III,III) complexes. Our investigations have been carried out using Pd_2(II,II) complex **1** because previous work has shown that complex **1** can be oxidized to isolable Pd_2(III,III) complexes upon treatment with appropriate two-electron oxidants.[3]

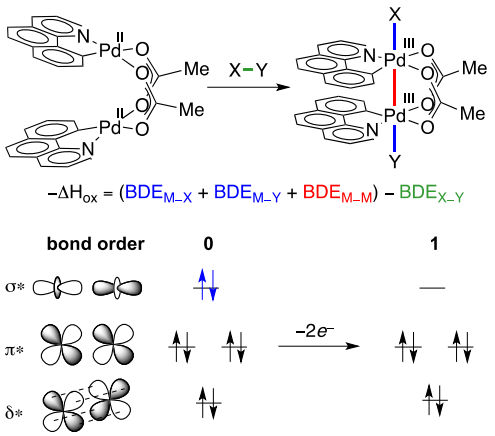

Figure 2. Nascent M–M bonding interactions in the oxidation transition state could facilitate bimetallic oxidation.

In targeting a transition state analog for the oxidation of a Pd_2(II,II) complex to a Pd_2(III,III) complex, we sought to identify an electron acceptor which would form a donor-acceptor complex with a Pd_2(II,II) complex without accomplishing formal metal-centered oxidation chemistry. Tetracyanoethylene (**2**) was selected based on its demonstrated ability to function as an acceptor to divalent Group 10 transition metal complexes, as well of its modest oxidation potential (E° = 0.13 V vs. SCE).[7] Treatment of Pd(II) complex **1** with 1.0 equivalents of tetracyanoethylene (TCNE; **2**), resulted in an immediate color change from pale yellow to dark blue (Scheme 1). Above 0 °C, the blue color slowly bleaches. The ^{1}H NMR spectrum of the blue solution resulting from treatment of **1** with **2** is consistent with the persistence of a binuclear complex; the observed ^{1}H NMR resonances are similar to those of Pd_2(II,II) complex **1**. A single crystal of dark-blue complex **3** was obtained by diffusion of toluene into a concentrated solution of **3** in CH_2Cl_2, and single crystal x-ray diffraction analysis established the interaction of Pd_2(II,II) complex **1** and **2**. In the solid state, a 2 : 1 adduct of **1** with **2** was observed, with close contact between the binuclear core of **1** and the olefinic carbon on **2** (Pd–C: 3.0332(3) Å). The binuclear core of **1** interacts with **2** at approximately a Burgi-Dunitz angle, consistent with interaction of the d_{z^2} orbitals of **1** interacting with the π* orbital of **2**.[8] The Pd–Pd distance contracts upon interaction of **1** (Pd–Pd: 2.84 Å (avg.)[9]) with **2** to afford complex **3** (Pd–Pd: 2.8028(5) Å), which is consistent with partial Pd–Pd bond formation upon binding of **1** to **2**. Interaction of the binuclear core of **1** with π-acid **2** as observed in the crystal structure of **3** resembles the early stages of the interaction of **1** with oxidants. The observed contraction from **1** to **3** is small relative to the contraction observed for oxidation of **1** to a Pd_2(III,III) complex, which is typically ~0.25 Å.[3]

Scheme 1. Treatment of Pd_2(II,II) complex **1** with **2** affords donor-acceptor complex **3**. ORTEP drawing of **3** with ellipsoids drawn at 50% probability (hydrogen atoms and solvent molecules removed for clarity). Selected distances in **3** [Å]: Pd(1)–Pd(2), 2.8028(2); Pd(1)–C(32), 3.0332(3).

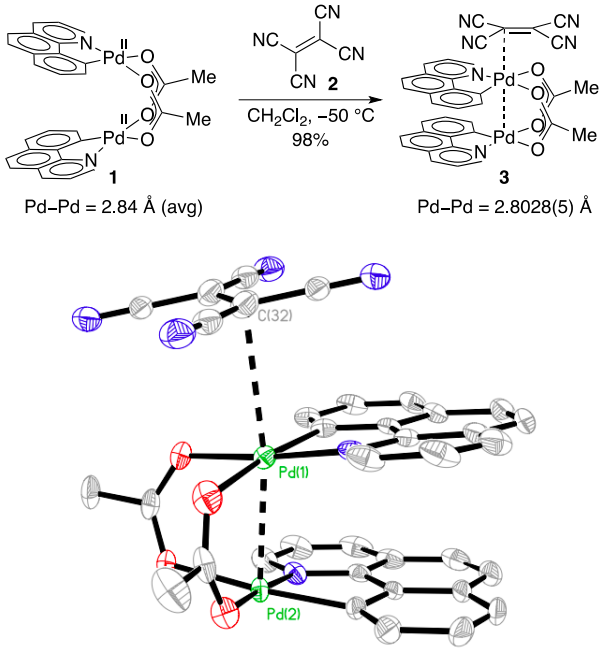

The electronic absorption spectrum of **3** displays bands which overlap with those of the electronic absorption spectra of **1** and **2**,[10] as well as a new broad absorbance band centered at λ_{max} = 680 nm (ε = 1600 M^{-1} cm^{-1}) (Fig. 3). While all of the electronic absorption features of **3** obey Beer's law in the presence of excess **2** (18.2 mM **2** in CH_2Cl_2), in the absence of excess **2**, the low-energy band in the absorption spectrum of **3** displays non-linear response to increasing concentration (Fig. 3 inset). Together, these observations suggest that the interaction of **1** and **2**, which gives rise to the absorption band at 680 nm, is reversible in solution. The equilibrium constant for the binding of **1** with **2** at 273 K (K_{eq} = [**3**]/[**1**][**2**]; [**1**] = [**2**] for **1** + **2** ⇆ **3**) was calculated to be 210 ± 30 based on the absorption spectra obtained in the absence of excess **2** and the molar absorptivity of **3**, which was determined in the presence of excess **2**. The equilibrium constant was computed based on both 1 : 1 and 2 :1 binding stoichiometries of **1** with **2**, with a better data fitting obtained for 1 : 1 binding.

The electronic structure of complex **3** and the orbital parentage of the absorption features observed for complex **3** were probed by time-dependent density functional theory (TD-DFT) calculations (Fig. 4).[11] Structures of both complexes **1** and **3** were optimized at the M06 level of DFT,[12] which has previously been shown to be robust for modeling binuclear Pd complexes,[3e,h,13] and the optimized geometries of **1** and **3** successfully described the crystallographically determined bond lengths and angles (computed Pd–Pd distance (Å): 2.87 (**1**), 2.84 (**3**). The low-energy absorption in the electronic

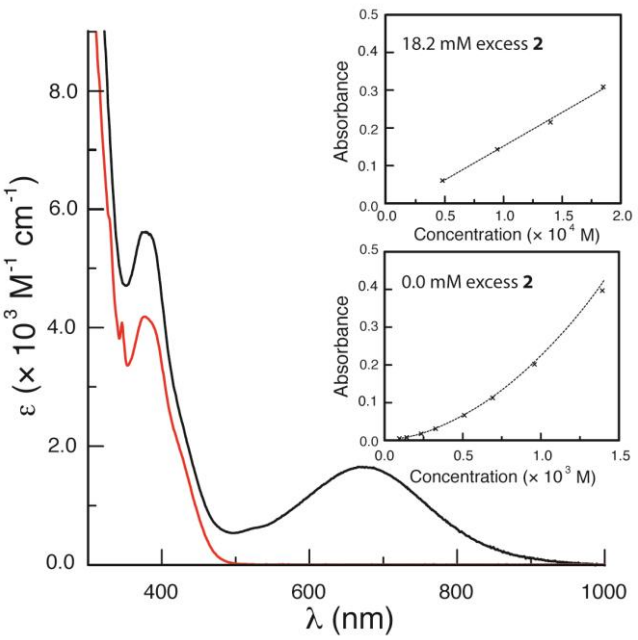

Figure 3. Extinction spectra of complex **1** (red) and charge-transfer complex **3** (black). Inset: In the presence of excess **2**, the charge transfer band (680 nm) of **3** obeys Beer's Law (top), while in the absence of excess **2**, non-linear absorption as a function of [**3**] is observed which is consistent with an equilibrium in which **3** interconverts with free **1** and **2** (bottom).

spectrum of complex **3** is primarily derived from HOMO to LUMO excitation. The HOMO of **3** is predominantly of Pd–Pd σ* parentage while the LUMO is dominated by the π* orbitals of **2**. As such, the low-energy band of **3** is assigned as a charge-transfer band between the binuclear core of **1** and the π* orbital of **2**.[14] This orbital interaction is the same as the interaction of binuclear Pd complexes with oxidants during the oxidation of Pd_2(II,II) complexes to Pd_2(III,III) complexes.[6,15] The low-energy absorbance in the spectrum of **3** differs from low energy absorbances frequently observed in binuclear Pd(III) complexes in that the HOMO of **3** is primarily the Pd–Pd σ^*, which in the LUMO of related Pd_2(III,III) complexes. The higher energy absorption features observed in the spectrum of **3**, as well as the features observed in the spectrum of **1**, are primarily ligand-based π to π* transitions. NBO[16] analysis of complexes **1** and **2** supports an increase in Pd–Pd bonding upon binding of **2** to **1**; calculated Pd–Pd bond orders for **1** and **2** reflect a small increase in the Pd–Pd bonding in **1** (Wiberg bond order: 0.1381 (**1**), 0.1402 (**3**); atom-atom overlap-weighted NAO bond order: 0.2604 (**1**), 0.2992 (**3**)).

In charge-transfer complex **3** there is direct interaction of the binuclear core of Pd_2(II,II) complex **1** with a tetracyanoethylene molecule. By selecting an appropriate acceptor, which is capable of interacting with the binuclear complex but insufficiently oxidizing to accomplish formal metal-centered oxidation to afford a Pd_2(III,III) complex, we have stabilized the binuclear core at an intermediate point along the reaction coordinate of oxidation of Pd_2(II,II) complexes to Pd_2(III,III) complexes. Similarly, donor-acceptor complexes between digold complexes and Lewis acids, which show contraction of the Au–Au distance, have been used to support the simultaneity of M–M bond formation and oxidation.[17] Pd–Pd contraction has also been observed in donor-acceptor complexes of Pd_2(II,II) complexes with the electron deficient Hg compound $Hg(C_6F_5)_2$ reported by Gabbaï.[18] The observation of M–M bond contraction along the reaction coordinate of oxidation suggests that Pd–Pd bond formation accompanies oxidation, and is thus capable of providing access to low-barrier pathways for metal-centered oxidation.

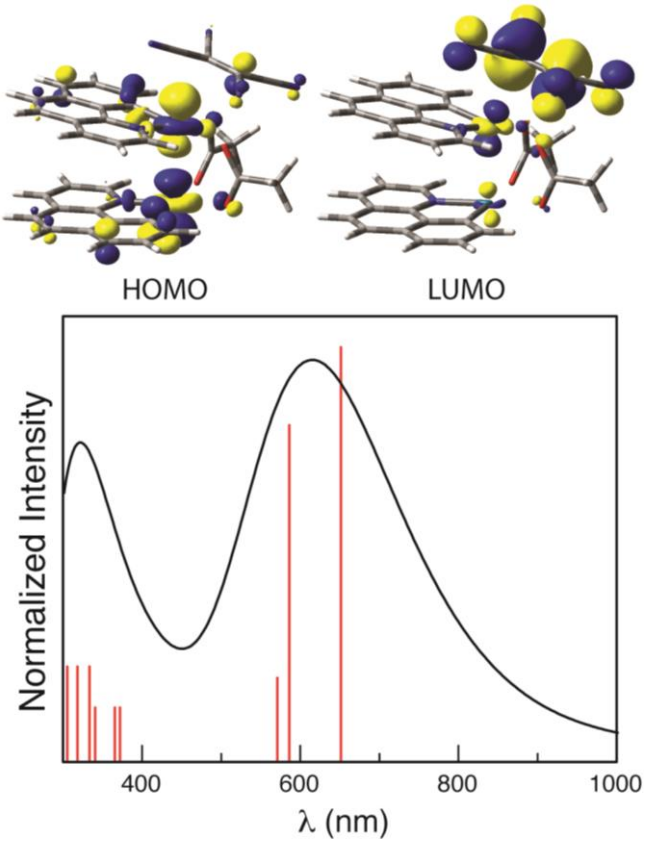

Figure 4. Calculated electronic absorption spectrum obtained from a TD-DFT calculation of structure **3** (black) and computed vertical excitations (red bars). The low-energy absorption in the spectrum of **3** is predominantly a HOMO to LUMO transition.

In summary, we report a transition state analog for the oxidation of a Pd_2(II,II) complex to a Pd_2(III,III) complex which was generated by interaction of the binuclear Pd core with an electron acceptor. The observed Pd–Pd contraction upon coordination of an electron acceptor is consistent with M–M bond contraction concurrent with oxidation, and suggests contraction along the M–M vector facilitates electron transfer by raising the dipalladium HOMO energy. The use of electron acceptors to probe geometrical perturbations during oxidation may find application in a variety of other oxidation mechanisms.

ASSOCIATED CONTENT

Supporting Information. Detailed procedures and characterization of new compounds, crystallographic data for **1** and **3**, computational details, and complete reference 11. This material is available free of charge via the Internet at http://pubs.acs.org.

AUTHOR INFORMATION

Corresponding Author

*E-mail: ritter@chemistry.harvard.edu

ACKNOWLEDGMENT

DFT computation was performed using the computer facilities at the Odyssey cluster at Harvard University. The authors thank Tamara M. Powers, Matthew B. Chambers, and Graham Sazama for helpful discussions and the National Science Foundation (CHE-0952753) and the Air Force (FA9550-10-1-0170) for financial support.

REFERENCES

(1) (a) Holm, R. H.; Kennepohl, P.; Solomon, E. I. *Chem. Rev.* **1996**, *96*, 2239-2314. (b) *Bioinorganic Catalysis*; Second ed.; Reedijk, J.; Bouwman, E., Eds.; Marcel Dekker, Inc.: New York, 1999. (c) *Biomimetic Oxidations Catalyzed by Transition Metal Complexes*; Meunier, B., Ed.; Imperial College Press: London, 2000. (d) Baik, M.-H.; Newcomb, M.; Friesner, R. A.; Lippard, S. J. *Chem. Rev.* **2003**, *103*, 2385-2419. (e) Tinberg, C. E.; Lippard, S. J. *Acc. Chem. Res.* **2011**, *44*, 280-288.

(2) (a) Wolfenden, R. *Acc. Chem. Res.* **1972**, *5*, 10-18. (b) Chook, Y. M.; Ke, H.; Lipscomb, W. N. *Proc. Nat. Acad. Sci.* **1993**, *90*, 8600-8603. (c) Schramm, V. L. *J. Biol. Chem.* **2007**, *282*, 28297-28300.

(3) (a) Powers, D. C.; Ritter, T. *Nat. Chem*. **2009**, *1*, 302-309; (b) Deprez, N. R.; Sanford, M. S. *J. Am. Chem. Soc.* **2009**, *131*, 11234-11241; (c) Powers, D. C.; Geibel, M. A. L.; Klein, J. E. M. N.; Ritter, T. *J. Am. Chem. Soc*. **2009**, *131*, 17050-17051; (d) Powers, D. C.; Xiao, D. Y.; Geibel, M. A. L.; Ritter, T. *J. Am. Chem. Soc*. **2010**, *132*, 14530-14536; (e) Powers, D. C.; Benitez, D.; Tkatchouk, E.; Goddard, W. A., III; Ritter, T. *J. Am. Chem. Soc*. **2010**, *132*, 14092-14103; (f) Powers, D. C.; Ritter, T. *Top. Organomet. Chem.* **2011**, *35*, 129-156. (g) Powers, D. C.; Ritter, T. *Acc. Chem. Res.* **2012**, *45*, 840-850. (h) Powers, D. C.; Lee, E.; Ariafard, A.; Sanford, M. S.; Yates, B. F.; Canty, A. J.; Ritter, T. *J. Am. Chem. Soc.* **2012**, *134*, 12002-12009.

(4) Disproportionation or mixed chloro-acetate binuclear Pd(III) complexes has recently been shown to afford symmetryical Pd_2(III,III) chloride and acetate complexes, with C–Cl reductive elimination proceding from a Pd_2(III,III) dichloride: Nielsen, M. C.; Lyngvi, E.; Schoenebeck, F. *J. Am. Chem. Soc.* **2013**, *asap*.

(5) Pd_2(II,II) complexes can show weak Pd–Pd bonding interactions: (a) Yip, H. K.; Lai, T. F.; Che, C. M. *J. Chem. Soc. Dalton Trans.* **1991**, 1639-1641. (b) Bercaw, J. E.; Durrell, A. C.; Gray, H. B.; Green, J. C.; Hazari, N.; Labinger, J. A.; Winkler, J. R. *Inorg. Chem.* **2010**, *48*, 1801-1810.

(6) (a) Cotton, F. A.; Murillo, C. A.; Walton, R. A.; eds. *Multiple Bonds Between Metal Atoms*; 3rd ed.; Springer Science and Business Media, Inc.: New York, 2005. (b) Umakoshi, K.; Sasaki, Y. *Adv. Inorg. Chem.* **1993**, *40*, 187-239. (c) Berry, J. F.; Cotton, F. A.; Ibragimov, S. A.; Murillo, C. A.; Wang, X. *Inorg. Chem.* **2005**, *44*, 6129-6137. (d) Cotton, F. A.; Gu, J.; Murillo, C. A.; Timmons, D. J. *J. Am. Chem. Soc.* **1998**, *120*, 13280-13281. (e) Cotton, F. A.; Koshevoy, I. O.; Lahuerta, P.; Murillo, C. A.; Sanaú, M.; Ubeda, M. A.; Zhao, Q. *J. Am. Chem. Soc.* **2006**, *128*, 13674-13675.

(7) (a) Yamamoto, T.; Yamamoto, A.; Ikeda, S. *J. Am. Chem. Soc.* **1971**, *93*, 3350-3359. (b) Fatiadi, A. J. *Synthesis* **1982**, 959-978. (c) Connelly, N. G.; Geiger, W. E. *Chem. Rev.* **1996**, *96*, 877-910.

(8) While the C=C bond of **2** is not substantially elongated upon interaction with **1**, pyrimidalization of the sp^2 carbon centers is observed (i.e the sum of the bond angles at C32 is 358.9 ± 0.8°). For discussion, see: Radhakrishnan, T. P.; Agranat, I. *Struct. Chem.* **1991**, *2*, 107-115.

(9) Two crystal morphologies of **1** have been isolated: CCDC 705005 and CCDC 832191, see Supporting Information for details.

(10) The absorption feature at 375nm in the spectrum of **3** is more intense than the corresponding feature in the spectrum of **1**, which may be due to the presence of new absorption modes in the visible spectrum of **3** involving participation of the orbitals of **2**, see Supporting Information for details.

(11) DFT calculations were executed using Gaussian 09: Frisch, M. J.; et al. *Gaussian 09*, revision A.02; Gaussian, Inc.: Wallingford, CT, **2009**.

(12) (a) Zhao, Y.; Truhlar, D. G. *Theor. Chem. Acc.* **2008**, *120*, 215-241. (b) Zhao, Y.; Truhlar, D. G. *Acc. Chem. Res.* **2008**, *41*, 157-167.

(13) (a) Ariafard, A.; Hyland, C. J. T.; Canty, A. J.; Sharma, M.; Brookes, N. J.; Yates, B. F. *Inorg. Chem.* **2010**, *49*, 11249-11253. (b) Ariafard, A.; Hyland, C. J. T.; Canty, A. J.; Sharma, M.; Yates, B. F. *Inorg. Chem.* **2011**, *50*, 6449-6457.

(14) (a) Mulliken, R. S. *J. Am. Chem. Soc.* **1952**, *74*, 811-824. (b) Steinmann, S. N.; Piemontesi, C.; Delachat, A.; Corminboef, C. *J. Chem. Theory Comput.* **2012**, *8*, 1629-1640.

(15) Canty, A. J.; Ariafard, A.; Sanford, M. S.; Yates, B. F. *Organometallics* **2013**, *asap*.

(16) (a) Reed, A. E.; Curtiss, L. A.; Weinhold, F. *Chem. Rev.* **1988**, *88*, 899–926. (b) Weinhold, F.; Landis, C. R. *Valency and Bonding: A Natural Bond Orbital Donor-Acceptor Perspective*; Cambridge University Press, 2005.

(17) (a) Usón, R.; Laguna, A.; Laguna, M.; Tartón, M. T.; Jones, P. G. *J. Chem. Soc., Chem. Commun.* **1988**, 740-741. (b) King, C.; Heinrich, D. D.; Garzon, G.; Wang, J.-C.; Fackler, J. P., Jr. *J. Am. Chem. Soc.* **1989**, *111*, 2300-2302. (c) Heinrich, D. D.; Staples, R. J.; Fackler, J. P., Jr. *Inorg. Chim. Acta* **1995**, *229*, 61-75. (d) Fackler, J. P., Jr. *Polyhedron* **1997**, *16*, 1-17.

(18) Kim, M.; Taylor, T. J.; Gabbaï, F. P. *J. Am. Chem. Soc.* **2008**, *130*, 6332-6333.

Biographical Information

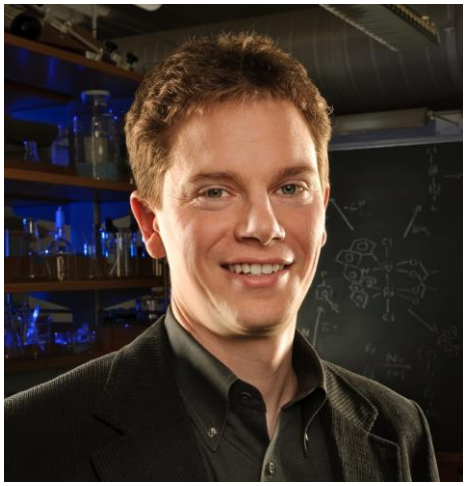

Tobias Ritter was appointed as Assistant Professor in the Department of Chemistry and Chemical Biology at Harvard in 2006 and promoted to Associate Professor in 2010. His research program is based on synthetic organic and organometallic chemistry with a focus on catalysis. The Ritter lab currently engages in the development of fluorination chemistry for late-stage functionalization of complex natural and unnatural products. Ritter studied in Braunschweig, Germany, Lausanne, Switzerland, Bordeaux, France, and Stanford, US. He performed undergraduate research with Prof. Barry M. Trost at Stanford, obtained his PhD working with Prof. Erick M. Carreira at ETH Zurich in 2004, and was a postdoc with Prof. Robert H. Grubbs at Caltech.

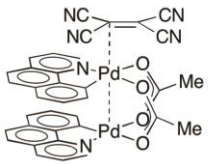

Pd–Pd Contraction in Donor-Acceptor Complex

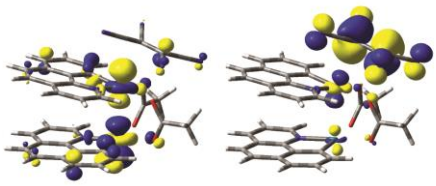

HOMO LUMO